



# Effect of the type of resin cement on the fracture resistance of chairside CAD-CAM materials after aging

Laura Vitória Rizzato<sup>1</sup>, Daniel Meneghetti<sup>2</sup>, Marielle Di Domênico<sup>1</sup>, Júlia Cadorin Facenda<sup>1,3</sup>, Katia Raquel Weber<sup>1,4\*</sup>, Pedro Henrique Corazza<sup>1</sup>, Márcia Borba<sup>1</sup>

<sup>1</sup>Graduate Program in Dentistry, University of Passo Fundo, Passo Fundo, RS, Brazil

<sup>2</sup>School of Dentistry, University of Passo Fundo, Passo Fundo, RS, Brazil

<sup>3</sup>Graduate Program in Dentistry, Federal University of Pelotas, Pelotas, RS, Brazil

<sup>4</sup>Department of Dentistry, School of Health Sciences, Positivo University, Curitiba, PR, Brazil

## ORCID

Laura Vitória Rizzato  
<https://orcid.org/0000-0002-8632-4692>

Daniel Meneghetti  
<https://orcid.org/0000-0002-4412-0501>

Marielle Di Domênico  
<https://orcid.org/0000-0002-2166-3052>

Júlia Cadorin Facenda  
<https://orcid.org/0000-0002-0575-6259>

Katia Raquel Weber  
<https://orcid.org/0000-0002-9919-7725>

Pedro Henrique Corazza  
<https://orcid.org/0000-0001-9480-1607>

Márcia Borba  
<https://orcid.org/0000-0001-7587-9839>

**PURPOSE.** The study objective was to evaluate the influence of the type of resin cement on the flexural strength and load to fracture of two chairside CAD-CAM materials after aging. **MATERIALS AND METHODS.** A polymer-infiltrated ceramic network (PICN) and a nanoceramic resin (RNC) were used to produce the specimens. Two types of dual-cure resin cements, a self-adhesive and a universal, were investigated. Bilayer specimens were produced (n = 10) and aged for 6 months in a humid environment before the biaxial flexural strength test ( $\sigma_f$ ). Bonded specimens were subjected to a mechanical aging protocol (50 N, 2 Hz, 37°C water, 500,000 cycles) before the compressive load test ( $L_f$ ).  $\sigma_f$  and  $L_f$  data were analyzed using two-way ANOVA and Tukey tests ( $\alpha = .05$ ). Chi-square test was used to analyze the relationship between failure mode and experimental group ( $\alpha = .05$ ). **RESULTS.** The type of resin cement and the interaction between factors had no effect on the  $\sigma_f$  and  $L_f$  of the specimens, while the type of restorative material was significant. RNC had higher  $\sigma_f$  and  $L_f$  than PICN. There was a significant association among the type of cracks identified for specimens tested in  $L_f$  and the restorative material. **CONCLUSION.** The type of resin cement had no effect on the flexural strength and load to fracture of the two investigated CAD-CAM chairside materials after aging. [J Adv Prosthodont 2023;15:136-44]

## KEYWORDS

CAD-CAM; Crown dental; Dental material; Properties; Resin cement

## Corresponding author

Katia Raquel Weber  
Number 1109, Apartment 39,  
Rogério Pereira de Camargo Street,  
Curitiba, Paraná (PR), Brazil  
Tel +(01155) 55 99643-0306  
E-mail  
katiaaraquelweber@hotmail.com

Received March 28, 2023 /  
Last Revision June 5, 2023 /  
Accepted June 20, 2023

## INTRODUCTION

Ceramics are widely used in prosthetic dentistry due to their great optical and mechanical properties, which allows the fabrication of restorations with good aesthetics, high color stability, excellent biocompatibility, low thermal con-

© 2023 The Korean Academy of Prosthodontics  
© This is an Open Access article distributed under the terms of the Creative Commons Attribution Non-Commercial License (<http://creativecommons.org/licenses/by-nc/4.0>) which permits unrestricted non-commercial use, distribution, and reproduction in any medium, provided the original work is properly cited.

ductivity and good resistance to fracture.<sup>1,2</sup> Nevertheless, the high elastic modulus and hardness, as well as the brittle behavior of ceramics, can compromise the longevity of the prosthetic rehabilitation.<sup>2,3</sup>

The search for more resilient and less stiff restorative materials combined with the consolidation of the computer-aided design and computer-aided manufacturing (CAD-CAM) technology in dentistry has led to the development of hybrid materials and high-performance polymers.<sup>2-5</sup> The first hybrid material introduced in dentistry was a polymer-infiltrated ceramic-network (PICN), which is composed of a dominant ceramic network infiltrated with a polymer matrix. The ceramic network has leucite as the major phase and zirconia as the minor phase.<sup>3-7</sup> The ceramic network provides resistance to deformation and wear, but it is brittle and susceptible to fracture; the polymer matrix is capable of plastic deformation, resulting in a more resilient material.<sup>5</sup> PICN have physical and mechanical properties similar to enamel and dentin.<sup>3,5,8,9</sup> This material has good flexural strength and fatigue resistance,<sup>10-16</sup> being indicated for crowns, veneers, inlays and onlays, and for patients with para-functional habits.<sup>4</sup>

The industrial production of CAD-CAM blocks also allowed the development of high-performance polymers. It is possible to fabricate composite materials with greater chemical stability and better physical and mechanical properties with greater incorporation of inorganic fillers and control of the degree of conversion of the polymer matrix.<sup>9,14,15,17</sup> For example, the nanoceramic resin (RNC) has 80 wt% of inorganic filler, being a mixture of zirconia particles (4 to 11 nm) and silica (20 nm). The remaining 20 wt% is composed of an organic matrix of highly cross-linked polymers containing predominantly urethane dimethacrylate (UDMA).<sup>7</sup> RNC has similar resilience to human dentin, good flexural strength, and good resistance to wear and staining.<sup>6,8,9,12-15,18</sup> This material is indicated for inlays, onlays and veneers.<sup>18</sup>

The introduction of these CAD-CAM restorative materials with different microstructure and composition raised doubts regarding which type of surface treatment, adhesive and cement can guarantee the longevity of the treatment.<sup>4,18-23</sup> Although most studies reported good bond strength results,<sup>19,20,22,23</sup> it is

important to characterize how the different bonding approaches affect the fracture resistance of these CAD-CAM restorative materials, especially after being subjected to conditions that simulate the oral environment. Additionally, the low stiffness of the RNC could result in restoration deflection and failures at the margins or debonding, which are failure modes reported clinically.<sup>9,17,21,24</sup> Therefore, tooth and implant-supported single crowns were removed from the RNC indications.<sup>17</sup>

Different types of resin cements are available to cement the restorations, being an important variable of the adhesive protocol.<sup>25</sup> Self-adhesive (SA) resin cements do not require acid-etching with phosphoric acid as they have acidic monomers in their composition, which promotes bonding by modifying the smear layer.<sup>26</sup> More recently, a combination of universal (U) resin cements and adhesives, that can be used in either self-etch, selective-etch or total-etch approach, were developed and represent a more versatile option to the dentist.<sup>27</sup> Nevertheless, the composition of the different restorative materials, cementation substrates, adhesives and cements, as well as the degradation effects of the oral environment, can significantly affect the clinical performance of the restorations, especially at the cementation interface.<sup>1,18-21,26,27</sup> Moreover, the thickness and elastic modulus of the resin cement layer influence the mechanical behavior of multilayer structures.<sup>28</sup>

Therefore, the objective of this study was to evaluate the effect of the type of resin cement, self-adhesive (SA) and universal (U), on the flexural strength and load to fracture of two chairside restorative CAD-CAM materials, PICN and RNC, after aging. The study hypotheses are: (1) the type of resin cement affect the biaxial flexural strength of bilayer specimens (restorative material + cement) after aging in a humid environment for 6 months; (2) the type of resin cement influences the fracture load of bonded specimens (substrate + cement + restorative material) after mechanical aging.

## MATERIALS AND METHODS

Two types of chairside CAD-CAM restorative materials were investigated, a polymer-infiltrated ceramic net-

work (PICN, Vita Enamic; Vita Zahnfabrik, Bad Sackingen, Germany) and a nanoceramic resin (RNC, Lava Ultimate; 3M Oral Care, St. Paul, MN, USA), and two types of dual-cure resin cements were used, a self-adhesive resin cement (SA, RelyX U200; 3M Oral Care, St. Paul, MN, USA) and an universal resin cement (U - RelyX Ultimate; 3M Oral Care, St. Paul, MN, USA). The mechanical behavior of the specimens was evaluated using a biaxial flexural strength test ( $\sigma_f$ ) after aging in a humid environment (specimens were immersed in distilled water for 6 months), and a compressive load test ( $L_f$ ) after mechanical aging (specimens were aged using a pneumatic mechanical cycling machine). For  $\sigma_f$ , bilayer specimens composed by the restorative material (1.0 mm) and the resin cement (- 0.05 mm) were produced. For  $L_f$ , the restorative material (1.0 mm) was cemented with resin cement (- 0.05 mm) to a dentin analog substrate (3.0 mm).

For the biaxial flexural strength test, disc shaped specimens of the two restorative materials were produced with 12 mm in diameter and 1 mm in thickness. First, CAD-CAM blocks were ground using a mechanical lathe (CA51H, FERDIMAT; São José dos Campos, Brazil) into 12 mm diameter cylinders, under water irrigation. Then, cylinders were cut into slices using a cutting machine (Miniton; Struers, Copenhagen, Denmark) with a diamond disc, under water irrigation. Specimens were ground and polished with silicon carbide papers (#300, #400, #600, #1200 grits) to produce 1 mm thick discs.

The surface treatment of the restorative materials are described in Table 1 and followed the manufacturer's recommendations, being acid-etch with 5% hydrofluoric acid for PICN and air-abrasion with 50  $\mu\text{m}$  alumina particles for RNC. All specimens were cleaned with distilled water and alcohol.

Subsequently, specimens of each restorative material were divided according to the type of resin cement used (SA and U) ( $n = 10$ ). The cementation protocol followed the manufacturer's recommendations for each cement (Table 1). For SA resin cement, a silane agent (Prosil; FGM, Joinville, SC, Brazil) was applied to the specimen surface and left to evaporate for 60 sec. For U resin cement, the specimen received a layer of a universal adhesive (Single Bond Universal; 3M Oral Care, St. Paul, MN, USA), which was applied with a microbrush for 20 sec, and light cured (Radium-cal; SDI, Sao Paulo, Brazil) for 20 sec.

The resin cement was applied to the specimen treated surface. A polyester strip was placed over the cement layer and the bilayer structure was inserted into a cementation device, in which a 750 g load was applied to guarantee a uniform cement layer. The excess of resin cement was removed using a microbrush. The cement was light cured (Radium-cal; SDI, Sao Paulo, Brazil) for 40 sec at each side of the multilayer specimen.

Specimens were stored for six months in distilled water at 37°C before the biaxial flexural strength test. Specimens were tested with the cement layer in tension using a piston-on-three-ball device (Biopdi, Sao Carlos, Brazil) (cement facing down the three spheres) in a universal testing machine (DL 2000, EMIC, Sao Jose dos Pinhais, Brazil), at 1 mm/min cross-head speed in 37°C distilled water. After the test, the fracture surface of specimens were analyzed using a stereomicroscope (STEMI 2000-C, ZEISS, Oberkochen, Germany) to measure the thickness of the restorative material and cement layer. The mean thickness of the cement layer was 55  $\mu\text{m}$  ( $\pm 37 \mu\text{m}$ ). The  $\sigma_f$  (MPa) of the multilayer specimen was calculated according to the bilayer equations below:<sup>29</sup>

**Table 1.** Surface treatment protocols

Restorative Material	Step 1	Resin Cement	Step 2
PICN	Acid-etch with 5% hydrofluoric acid for 60 sec	SA (self-adhesive)	Silane agent for 60 sec
		U (universal)	Universal adhesive for 20 sec + light curing for 20 sec
RNC	Air-abrasion with 50 $\mu\text{m}$ $\text{Al}_2\text{O}_3$ particles at 2 bar pressure (30 psi)	SA (self-adhesive)	Silane agent for 60 sec
		U (universal)	Universal adhesive for 20 sec + light curing for 20 sec

PICN, polymer-infiltrated ceramic network; RNC, nanoceramic resin.

$$\sigma_1 = \frac{-E_1(z - z^*)P}{8\pi(1 - \nu_1)D^*} \left\{ 1 + 2 \ln \left( \frac{a}{c} \right) + \frac{1 - \nu}{1 + \nu} \left[ 1 - \frac{c^2}{2a^2} \right] \frac{a^2}{R^2} \right\} \text{ (for } 0 \leq z \leq t_1 \text{ and } r \leq c)$$

$$\sigma_2 = \frac{-E_2(z - z^*)P}{8\pi(1 - \nu_2)D^*} \left\{ 1 + 2 \ln \left( \frac{a}{c} \right) + \frac{1 - \nu}{1 + \nu} \left[ 1 - \frac{c^2}{2a^2} \right] \frac{a^2}{R^2} \right\} \text{ (for } t_1 \leq z \leq t_1 + t_2 \text{ and } r \leq c)$$

where,  $z^*$ ,  $D^*$  and  $\nu$  are:

$$z^* = \frac{\frac{E_1 t_1^2}{2(1 - \nu_1^2)} + \frac{E_2 t_2^2}{2(1 - \nu_2^2)} + \frac{E_2 t_1 t_2}{(1 - \nu_2^2)}}{\frac{E_1 t_1}{(1 - \nu_1^2)} + \frac{E_2 t_2}{(1 - \nu_2^2)}}$$

$$D^* = \frac{E_1 t_1^3}{3(1 - \nu_1^2)} + \frac{E_2 t_2^2}{3(1 - \nu_2^2)} + \frac{E_2 t_1 t_2 (t_1 + t_2)}{(1 - \nu_2^2)} - \frac{\left[ \frac{E_1 t_1^2}{2(1 - \nu_1^2)} + \frac{E_2 t_2^2}{2(1 - \nu_2^2)} + \frac{E_2 t_1 t_2}{(1 - \nu_2^2)} \right]^2}{\frac{E_1 t_1}{(1 - \nu_1^2)} + \frac{E_2 t_2}{(1 - \nu_2^2)}}$$

$$\nu = \frac{\nu_1 t_1 + \nu_2 t_2}{t_1 + t_2}$$

where:  $a$  is the radius of the specimen support circle (5 mm),  $c$  is the piston radius (0.775 mm),  $D$  is the specimen diameter (- 12 mm),  $R$  is specimen radius (- 6 mm),  $t_1$  is the thickness of the cement layer (- 0.05 mm),  $t_2$  is the thickness of the restorative material (- 1.0 mm),  $E_1$  is the elastic modulus of the resin cement,  $E_2$  is the elastic modulus of the restorative material,  $P$  is the fracture load (N),  $\nu_1$  is the Poisson's ration of the resin cement, and  $\nu_2$  is the Poisson's ratio of the restorative material.

In the equation,  $E = 12.7$  GPa and  $\nu = 0.47$  for RNC;<sup>7</sup>  $E = 37.4$  GPa and  $\nu = 0.26$  for PICN;<sup>7</sup>  $E = 7.7$  GPa for resin cement U;  $E = 6.6$  GPa for resin cement SA;  $\nu = 0.5$  for the two resin cements (information provided by the manufacturer).<sup>7</sup>

The fracture surface of the specimens was analyzed following the principles of fractography to identify the fracture origin, using a stereomicroscope. Two specimens of each experimental group were selected for a detailed analysis of the fracture surface using a scanning electron microscope (SEM-Model Vega 3; TESCAN, Brno, Czechoslovakia). For the SEM analysis, the specimens were cleaned in an ultrasonic bath

with 90% alcohol and gold-sputtered.

For the compressive load test, plate-shaped specimens of PICN and RNC were produced by cutting CAD-CAM blocks using a cutting machine (Miniton; Struers, Copenhagen, Denmark) and a diamond disc, under water irrigation. Specimens were ground and polished with silicon carbide papers (#300, #400, #600, #1200 grit size) to produce plates of 1 mm thickness (10 × 12 mm).

Discs of a dentin analog substrate (glass fiber-reinforced epoxy resin, NEMA G10; International Paper, Hampton, SC, USA) with 2 mm thickness were obtained by cutting the rods of G10 material and griding with #400 grit silicon carbide paper. Prior to cementation, the surface of G10 was etched with 10% hydrofluoric acid (Condac porcelain; FGM, Joinville, SC, Brazil) for 60 sec, washed with water, and air-dried and a silane agent was applied for 60 sec (Prosil; FGM, Joinville, SC, Brazil). G10 is a fiber-reinforced epoxy resin with elastic and adhesive properties similar to dentin.<sup>11,18,30,31</sup> Acid etching is recommended to produce micro retentions for adhesive bonding.<sup>31</sup>

The restorative materials were further divided ac-

ording to the type of resin cement (SA and U) ( $n = 10$ ). Cementation of the restorative materials to the dentin analog substrate followed the same protocol described for the  $\sigma_f$  specimens reported previously (Table 1).<sup>11,18,30</sup> Cemented specimens were stored in distilled water at 37°C for 48 hr.

Before the compressive load test, specimens were subjected to an aging protocol using a pneumatic mechanical cycling machine (Biocycle mechanical cyler; BioPDI, São Paulo, Brazil). A 50 N load was applied to the restorative material surface by a flat metallic piston (3 mm diameter contact area stainless steel piston) with a frequency of 2 Hz, in 37°C distilled water, for 500,000 cycles. A flat piston was used to guarantee a uniform contact area and pressure during aging.<sup>11,30,32</sup>

The compressive load test ( $L_f$ ) was performed using a universal testing machine (Instron 23-10, series 2310P-0008; Instron, São José dos Pinhais, PR, Brazil) in 37°C distilled water. A compressive load was applied to the center of the cemented specimen by the flat metallic piston (3 mm diameter contact area) with a cross-head speed of 0.5 mm/min. An amplified microphone was connected to the universal testing machine and to a computer. Load application was acoustically monitored by using a software (Audacity Sound Editor; Free Software Foundation, Boston, MA, USA). The test was interrupted at the sound of the first crack, shown in the software as a sharp sound wave, and the load was recorded ( $L_f$  in N).<sup>11,18,32,33</sup>

Specimens were analyzed using transillumination with blue light after the mechanical aging protocol and after the compressive load test in order to identify cracks and fractures. Cracks were classified as: radial, when initiating from the intaglio surface of

the restorative material; cone, which are ring-shaped cracks initiating from the surface of the restorative material in contact with the loading piston; and combined, when both radial and cone cracks are identified.<sup>11,18,30,33</sup>

Fracture load and flexural strength data passed the Shapiro-Wilk Normality test and the similar variance test ( $P > .05$ ). Two-way ANOVA (factor 1: restorative material, factor 2: resin cement) and Tukey tests were used to analyze  $\sigma_f$  and  $L_f$  data ( $\alpha = .05$ ). Chi-square test was used to analyze the relationship between the type of crack identified for specimens tested in compressive load and the experimental group ( $\alpha = .05$ ).

## RESULTS

For biaxial flexural strength, the factor of restorative material was statistically significant ( $P < .001$ ;  $\beta = 0.99$ ). Yet, the factor of resin cement type ( $P = .463$ ;  $\beta = 0.05$ ) and the interaction between factors ( $P = .058$ ;  $\beta = 0.36$ ) were not statistically significant. RNC had higher  $\sigma_f$  than PICN (Table 2). Fractographic analysis of the bilayer specimens indicated that the fracture origin was located on the surface of the cement layer and propagated throughout the restorative material for all experimental groups. Representative images of the fracture surface of RNC and PICN bilayer specimens that failed in flexure are shown in Figure 1.

The factor of resin cement type ( $P = .250$ ;  $\beta = 0.08$ ) and the interaction between factors ( $P = .057$ ;  $\beta = 0.36$ ) were not statistically significant for fracture load of bonded specimens. The factor of restorative material was statistically significant ( $P < .001$ ;  $\beta = 1.00$ ). RNC showed higher  $L_f$  than PICN, as shown in Table 2.

No specimen failed or debonded from the substrate

**Table 2.** Mean (standard deviation) values of biaxial flexural strength ( $\sigma_f$  - MPa) and fracture load ( $L_f$  - N) for the experimental groups

Restorative Material	Resin Cement			
	$\sigma_f$ - MPa		$L_f$ - N	
	U	SA	U	SA
PICN	98 (7) <sup>b</sup>	111 (9) <sup>b</sup>	1578 (730) <sup>b</sup>	2159 (423) <sup>b</sup>
RNC	129 (12) <sup>a</sup>	123 (25) <sup>a</sup>	3905 (614) <sup>a</sup>	3758 (536) <sup>a</sup>

Means followed by similar letters in the same column are statistically similar ( $P \geq .05$ ).

PICN, polymer-infiltrated ceramic network; RNC, nanoceramic resin; SA, self-adhesive; U, universal.

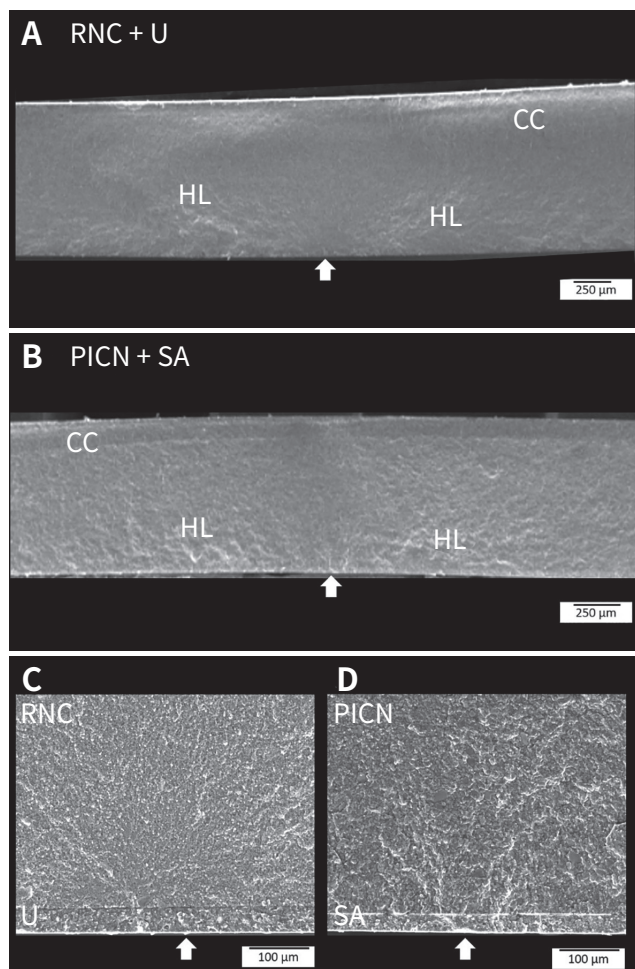


**Fig. 1.** Representative SEM images of the fracture surface of bilayer specimens tested for biaxial flexural strength: (A) RNC combined with U resin cement; (B) PICN combined with SA resin cement; (C) closer view of the fracture origin of the specimen shown in image a (RNC+U); (D) closer view of the fracture origin of the specimen shown in image b (PICN+SA). Compression curl (CC) and hackle lines (HL) indicate the direction of crack propagation from the bottom to the top of the specimen fracture surface. White arrows point to the origin of the fracture on the surface of the cement layer.

SEM, scanning electron microscope; PICN, polymer-infiltrated ceramic network; RNC, nanoceramic resin; SA, self-adhesive; U, universal.

during mechanical aging. The failure mode for specimens tested in compressive load was cracking, as shown in Figure 2. Fractures of the restorative materials were not observed. A significant relationship was found between the type of crack and the experimental group ( $P = .003$ ). RNC specimens had a higher frequen-

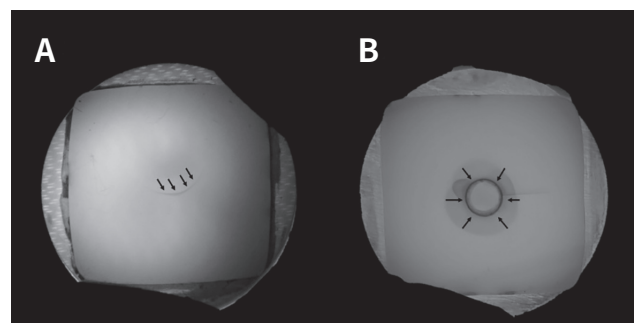


**Fig. 2.** Images of the fracture surface of specimens tested in compression, using transillumination: (A) black arrows point to a radial crack located in the specimen intaglio surface, at the cementation interface with the dentin analog; (B) black arrows point to a cone crack located in the specimen surface in contact with the loading piston.

cy of cone cracks (90%), while PICN specimens had a higher frequency of combined (50%) and radial (25%) cracks, regardless of the type of resin cement used.

## DISCUSSION

A wide variety of restorative CAD-CAM materials are available to rehabilitate patients. Among these materials are PICN and RNC, which have mechanical properties that are suitable for clinical use, being less stiff and more resilient than ceramics.<sup>4,7,17</sup> Several cementation strategies are available, with different surface treatments, adhesives and resin cements,<sup>18-22,26,27</sup> and it is important to understand how they may affect the structure's resistance to fracture. Therefore, the present study focused on the mechanical characterization of chairside CAD-CAM materials combined with different resin cements and subjected to conditions that simulate the oral environment, aiming to support the cementation protocols used in the clinic.

The type of resin cement had no effect on the biaxial flexural strength of bilayer specimens after aging in a humid environment for 6 months, rejecting the first hypothesis of the study. The resin cements evaluated have similar inorganic filler content (~43%), which lead to similar mechanical properties as well. The manufacturer (3M Oral Care) reported flexural strength values of 98 MPa for the universal resin ce-

ment and 99 MPa for the self-adhesive. In addition, an *in vitro* study found compressive strength of 293 MPa for the universal and 283 MPa for the self-adhesive.<sup>25</sup> Moreover, although self-adhesive resin cements are more hydrophilic,<sup>26</sup> when specimens were analyzed using microscopy, after 6 months of water storage, it was not possible to identify characteristics of cement degradation (i.e. heterogeneous areas that indicate loss of material).

When the two CAD-CAM materials were compared, RNC showed superior flexural strength than PICN, regardless of the type of resin cement used. PICN has a greater ceramic content, which provides greater resistance to deformation and wear, while increasing the material brittleness.<sup>5-7,9,12,14</sup> On the contrary, RNC has a greater polymer content, which absorbs the applied loads and increases the material resistance to fracture.<sup>6-8,12,14,17</sup> Previous studies found higher flexural strength values for RNC when compared to PICN, corroborating with our results.<sup>8,9,14,16</sup> Fractography of bilayer specimens showed similar failure pattern for all experimental groups, with crack initiating at the surface of the resin cement layer subjected to tensile stresses during the biaxial flexure test and propagating through the restorative material.

The second study hypothesis was rejected as the type of resin cement had no influence on the fracture load of bonded specimens subjected to mechanical aging. The resin cement elastic modulus (E) could affect the stress distribution of bonded specimens (substrate + resin cement + restorative material).<sup>11,28</sup> Nevertheless, in the present study, due to the small thickness (~ 55  $\mu\text{m}$ ) of the cement layer, differences in the elastic properties of the two resin cements ( $E_U = 7.7 \text{ GPa}$ ;  $E_{SA} = 6.6 \text{ GPa}$ ) did not significantly affect the mechanical behavior of the multilayer structure. Moreover, the absence of debonding during mechanical aging suggest good adhesion between restorative material, cement and substrate, as reported in previous studies.<sup>11,18</sup>

For the fracture load test, RNC also showed higher values than PICN. The superior mechanical behavior of RNC bonded specimens can be attributed to the greater flexural strength of the restorative material and the similarity among the elastic properties of RNC, resin cement, and dentin analog substrate.<sup>11,18,28</sup>

A small mismatch between the E values of different materials in a multilayer structure results in a more uniform stress distribution across the layers when the structure is tested in compression.<sup>28</sup>

Moreover, a study that evaluated the mechanical behavior of PICN and an indirect composite resin bonded with a universal resin cement to a dentin analog concluded that the structure could be reinforced if the substrate has a higher elastic modulus than the restorative material.<sup>11</sup> The elastic modulus of the dentin analog substrate ( $E = 13.1 \text{ GPa}$ ) is slightly superior to that of the RNC ( $E = 12.7 \text{ GPa}$ ),<sup>7,31</sup> which results in the suppression of tensile stresses at the restorative material intaglio surface. Higher stress concentration is located at the surface of the restorative material in contact with the loading piston, leading to cone cracks, which were responsible for 90% of RNC failures.<sup>11,18,33</sup>

On the contrary, if the restorative material has a greater elastic modulus than the substrate, such as PICN material ( $E = 37.4 \text{ GPa}$ ),<sup>7</sup> high tensile stresses are located at the intaglio surface due to the substrate flexure under compressive loading, generating radial cracks.<sup>11,30,33</sup> Nevertheless, studies have shown that radial and cone cracks are competing failure modes.<sup>11,18,28,30,32,33</sup> Factors including the load level used in the mechanical test;<sup>30,32,33</sup> thickness of the substrate, cement and restorative material;<sup>28,33</sup> type of material, size and shape of the loading piston;<sup>30,32,33</sup> and, type of supporting substrate<sup>11,28,33</sup> can affect the stress distribution and failure mode of bonded structures as well. Moreover, mechanical aging can also contribute to accumulate damage at the contact surface, resulting in combined failure modes.<sup>11,30,32,33</sup>

Multilayer structures were evaluated, aiming to simulate the configuration of a single crown bonded with resin cement to the dental substrate;<sup>11,18,30,31,33</sup> however, the use of a simplified structure, which does not correspond to the complex geometry of a prosthesis, is a study limitation. The compressive load test of bonded specimens was planned as to create the same crack system reported for clinical failures of prosthetic restorations.<sup>33</sup> Clinical extrapolations should also consider that a total etch protocol was used for both resin cements, as the literature recommends acid-etching the dentin analog substrate.<sup>31</sup>

The surface treatments prior to bonding followed the manufacturer recommendations for each restorative material, being etched with hydrofluoric acid for PICN and air-abraded with particles for RNC.<sup>23</sup> Nevertheless, the oral environment was simulated by mechanical aging the bonded structures in water at 37°C with 50 N load and 2 Hz frequency.<sup>11-13,30</sup>

## CONCLUSION

The type of resin cement had no effect on the flexural strength and load to fracture of cemented CAD-CAM restorative materials after aging. The nanoceramic resin had greater mechanical behavior than PICN.

## ACKNOWLEDGMENTS

The authors thank PIBIC/CNPq (118864/2018-1), PROBIC/FAPERGS, CAPES (Finance Code 001).

## REFERENCES

1. Sonza QN, Della Bona A, Pecho OE, Borba M. Effect of substrate and cement on the final color of zirconia-based all-ceramic crowns. *J Esthet Restor Dent* 2021;33:891-8.
2. Silva LHD, Lima E, Miranda RBP, Favero SS, Lohbauer U, Cesar PF. Dental ceramics: a review of new materials and processing methods. *Braz Oral Res* 2017;31:e58.
3. Della Bona A, Corazza PH, Zhang Y. Characterization of a polymer-infiltrated ceramic-network material. *Dent Mater* 2014;30:564-9.
4. Facenda JC, Borba M, Corazza PH. A literature review on the new polymer-infiltrated ceramic-network material (PICN). *J Esthet Restor Dent* 2018;30:281-6.
5. Coldea A, Swain MV, Thiel N. Mechanical properties of polymer-infiltrated-ceramic-network materials. *Dent Mater* 2013;29:419-26.
6. Coldea A, Fischer J, Swain MV, Thiel N. Damage tolerance of indirect restorative materials (including PICN) after simulated bur adjustments. *Dent Mater* 2015;31:684-94.
7. Belli R, Wendler M, de Ligny D, Cicconi MR, Petschelt A, Peterlik H, Lohbauer U. Chairside CAD/CAM materials. Part 1: Measurement of elastic constants and microstructural characterization. *Dent Mater* 2017;33:84-98.
8. Choi BJ, Yoon S, Im YW, Lee JH, Jung HJ, Lee HH. Uniaxial/biaxial flexure strengths and elastic properties of resin-composite block materials for CAD/CAM. *Dent Mater* 2019;35:389-401.
9. Awada A, Nathanson D. Mechanical properties of resin-ceramic CAD/CAM restorative materials. *J Prosthet Dent* 2015;114:587-93.
10. El Zhawi H, Kaizer MR, Chughtai A, Moraes RR, Zhang Y. Polymer infiltrated ceramic network structures for resistance to fatigue fracture and wear. *Dent Mater* 2016;32:1352-61.
11. Facenda JC, Borba M, Benetti P, Della Bona A, Corazza PH. Effect of supporting substrate on the failure behavior of a polymer-infiltrated ceramic network material. *J Prosthet Dent* 2019;121:929-34.
12. Wendler M, Kaizer MR, Belli R, Lohbauer U, Zhang Y. Sliding contact wear and subsurface damage of CAD/CAM materials against zirconia. *Dent Mater* 2020;36:387-401.
13. Aboushelib MN, Elsafi MH. Survival of resin infiltrated ceramics under influence of fatigue. *Dent Mater* 2016;32:529-34.
14. Stawarczyk B, Liebermann A, Eichberger M, Güth JF. Evaluation of mechanical and optical behavior of current esthetic dental restorative CAD/CAM composites. *J Mech Behav Biomed Mater* 2015;55:1-11.
15. Mörmann WH, Stawarczyk B, Ender A, Sener B, Attin T, Mehl A. Wear characteristics of current aesthetic dental restorative CAD/CAM materials: two-body wear, gloss retention, roughness and Martens hardness. *J Mech Behav Biomed Mater* 2013;20:113-25.
16. Wendler M, Belli R, Petschelt A, Mevec D, Harrer W, Lube T, Danzer R, Lohbauer U. Chairside CAD/CAM materials. Part 2: Flexural strength testing. *Dent Mater* 2017;33:99-109.
17. Mainjot AK, Dupont NM, Oudkerk JC, Dewael TY, Sadoun MJ. From artisanal to CAD/CAM blocks: State of the art of indirect composites. *J Dent Res* 2016;95:487-95.
18. Nogueira AD, Corazza PH, Pecho OE, Perez MM, Borba M. Effect of cementation on the mechanical behavior of a nanoceramic resin. *Cerâmica* 2020;66:236-42.
19. Lührs AK, Pongprueksa P, De Munck J, Geurtsen W, Van Meerbeek B. Curing mode affects bond strength of adhesively luted composite CAD/CAM restorations



- to dentin. *Dent Mater* 2014;30:281-91.
20. Flury S, Schmidt SZ, Peutzfeldt A, Lussi A. Dentin bond strength of two resin-ceramic computer-aided design/computer-aided manufacturing (CAD/CAM) materials and five cements after six months storage. *Dent Mater J* 2016;35:728-35.
  21. Canatan S, Oz FD, Bolay S. A randomized, controlled clinical evaluation of two resin cement systems in the adhesion of CAD/CAM-fabricated resin nanoceramic restorations: 18-month preliminary results. *J Esthet Restor Dent* 2022;34:1005-14.
  22. Bello YD, Di Domenico MB, Magro LD, Lise MW, Corazza PH. Bond strength between composite repair and polymer-infiltrated ceramic-network material: Effect of different surface treatments. *J Esthet Restor Dent*. 2019;31:275-9.
  23. Castro EF, Azevedo VLB, Nima G, Andrade OS, Dias CTDS, Giannini M. Adhesion, Mechanical properties, and microstructure of resin-matrix CAD-CAM ceramics. *J Adhes Dent* 2020;22:421-31.
  24. Oz FD, Bolay S, Canatan S. A clinical evaluation of resin nanoceramic CEREC Omnicam restorations associated with several factors. *J Esthet Restor Dent* 2021; 33:583-9.
  25. Rohr N, Fischer J. Effect of aging and curing mode on the compressive and indirect tensile strength of resin composite cements. *Head Face Med* 2017;13:22.
  26. Manso AP, Carvalho RM. Dental cements for luting and bonding restorations: Self-adhesive resin cements. *Dent Clin North Am* 2017;61:821-34.
  27. Cuevas-Suárez CE, da Rosa WLO, Lund RG, da Silva AF, Piva E. Bonding performance of universal adhesives: an updated systematic review and meta-analysis. *J Adhes Dent* 2019;21:7-26.
  28. Ma L, Guess PC, Zhang Y. Load-bearing properties of minimal-invasive monolithic lithium disilicate and zirconia occlusal onlays: finite element and theoretical analyses. *Dent Mater* 2013;29:742-51.
  29. Borba M, de Araújo MD, de Lima E, Yoshimura HN, Cesar PF, Griggs JA, Della Bona A. Flexural strength and failure modes of layered ceramic structures. *Dent Mater* 2011;27:1259-66.
  30. Weber KR, Meneghetti DE, Benetti P, Della Bona A, Griggs JA, Borba M. Influence of piston material on the fatigue behavior of a glass-ceramic. *J Prosthet Dent* 2023;129:931-7.
  31. Merlo EG, Della Bona A, Griggs JA, Jodha KS, Corazza PH. Mechanical behavior and adhesive potential of glass fiber-reinforced resin-based composites for use as dentin analogues. *Am J Dent* 2020;33:310-4.
  32. Lana TMDS, Weber KR, Medeiros JA, Goedel F, Benetti P, Borba M. Fatigue-life and stress distribution of a glass-ceramic under different loading conditions. *Braz Dent J* 2023;34:80-8.
  33. Kelly JR, Rungruanganunt P, Hunter B, Vailati F. Development of a clinically validated bulk failure test for ceramic crowns. *J Prosthet Dent* 2010;104:228-38.